Prolongation of the Lifetime of the Charge-Separated State at Low Temperatures in a Photoinduced Electron-Transfer System of [60]Fullerene and Ferrocene Moieties Tethered by Rotaxane Structures

G. Abraham Rajkumar,[†] Atula S. D. Sandanayaka,[‡] Kei-ichiro Ikeshita,[¶] Yasuyuki Araki,[‡] Yoshio Furusho,[£] Toshikazu Takata,*[,†] and Osamu Ito*[,‡]

Department of Organic and Polymeric Materials, Tokyo Institute of Technology, Ookayama 2-12-1, Meguro, Tokyo 152-8552, Japan, Institute of Multidisciplinary Research for Advanced Materials, Tohoku University, Katahira, Aoba-ku, Sendai 980-8577, Japan, Department of Applied Chemistry, Graduate School of Engineering, Osaka Prefecture University, Sakai, Osaka 599-8531, Japan, and Yashima Super-Structured Helix Project, JST, Moriyama-ku, Nagoya 552-8555, Japan

Received: November 19, 2005; In Final Form: February 13, 2006

A rotaxane tethering both fullerene (C_{60}) and ferrocene (Fc) moieties (abbreviated as $(C_{60};Fc)_{rotax+}$) was synthesized in a good yield by the urethane end-capping of pseudorotaxane based on the crown ether−secondary amine motif. In $(C_{60};Fc)_{rotax+}$, the C_{60} group serving as an electron acceptor is attached to the crown ether wheel, through which the axle with a Fc group acting as an electron donor on its end penetrates. The intrarotaxane photoinduced energy-transfer and electron-transfer processes between C_{60} and Fc in $(C_{60};Fc)_{rotax+}$ have been investigated by time-resolved transient absorption and fluorescence measurements with changing solvent polarity. Nanosecond transient absorption measurements of the rotaxane demonstrated that the charge-separated state $(C_{60}^{\bullet-};Fc^{\bullet+})_{rotax+}$ is formed mainly via the excited triplet state of C_{60} in polar solvents. The lifetime of $(C_{60}^{\bullet-};Fc^{\bullet+})_{rotax+}$ was evaluated to be 20 ns in dimethylformamide (DMF) at room temperature. With lowing temperature, the lifetime of $(C_{60}^{\bullet-};Fc^{\bullet+})_{rotax+}$ extends to 270 ns in DMF at −65 °C, due to the structural changes leaving $C_{60}^{\bullet-}$ and $Fc^{\bullet+}$ at a relatively long distance in the low-temperature region.

Introduction

The design of supramolecular logic elements has recently been recognized as being quite important for molecular-scale photonic devices.[1−3] These components may permit access to the complex photophysical processes, such as energy transfer (EN), energy migration, and optical switching.[4] Thus, supramolecular photochemistry has progressively enlarged the spectrum of interest toward light-driven molecular machines, molecular switches and sensors, and molecular electronics, thus reaching the crossroad between chemistry, biology, and information technology.[5−8] Fundamental studies of supramolecular photochemistry are also relevant to biological studies of vision and photosynthesis.[9] The excited-state properties of fullerene derivatives in the supramolecules have attracted interest in studies of photosynthesis models, as well as in studies of new photovoltaic devices and photodetectors.[10,11]

Various covalently bonded C_{60}-based donor−acceptor systems involving electron-mediating and hole-transfer reagents have been extensively studied in order to establish rapid and efficient charge separation (CS) via the excited singlet state of fullerene derivatives and donor molecules, resulting in long lifetimes of the CS states due to slow charge recombination (CR).[12−16] Supramolecules composed of a fullerene coordinated to the axial of zinc porphyrins have also been shown to display a fast and effective CS process via the excited singlet states of the fullerene and porphyrin components.[17−21]

Recently, rotaxanes containing fullerenes as electron acceptors and phthalocyanine and porphyrin as electron donors were synthesized, whereby fullerenes were spatially fixed with respect to the phthalocyanine and porphyrin moieties. In these rotaxanes, it was reported that the through-space CS process takes place via the singlet and triplet excited states of these chromophores, depending on the distance between the donor and the acceptor.[22,23] In rotaxanes with distant electron donors and acceptors, through-space CS usually tends to take place via the excited triplet state of the components. This tendency seems to contrast the covalently bonded donor−acceptor systems, in which the CS usually takes place via the excited singlet state with a through-bond mechanism. Furthermore, it has been pointed out that the fluctuation of the relative distance between the donor and the acceptor plays an important role in the electron transfer (ET) process in rotaxane.[24]

In the present study, we synthesized a rotaxane containing both a [60]fullerene (C_{60}) moiety as an electron acceptor and a ferrocene (Fc) moiety as an electron donor. Figure 1 shows the structures of the rotaxane (abbreviated as $(C_{60};Fc)_{rotax+}$), in which the axle connecting the Fc donor moiety at the one end penetrates through the crown ether wheel attached to the C_{60} acceptor. $(C_{60};Fc)_{rotax+}$ has a positive charge on the nitrogen atom in the middle of the axle, which is expected to interact with the oxygen atoms of the crown ether, probably fixing the C_{60} and Fc moieties in a certain spatial arrangement. $(C_{60};Fc)_{rotax+}$

* Authors for correspondence. E-mail: ttakata@polymer.titech.ac.jp (T.T.); ito@tagen.tohoku.ac.jp (O.I.).
[†] Tokyo Institute of Technology.
[‡] Tohoku University.
[¶] Osaka Prefecture University.
[£] Yashima Super-Structured Helix Project.

10.1021/jp056699i CCC: $33.50
Published on Web 03/11/2006

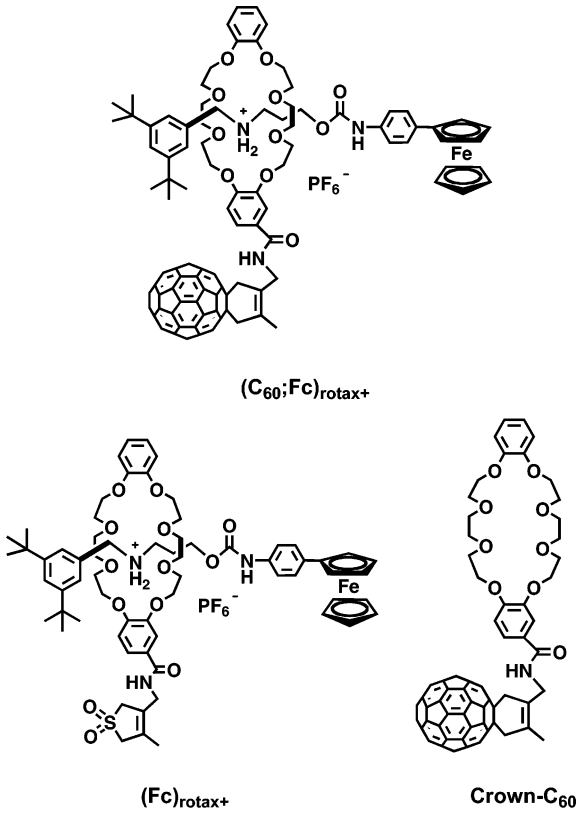

Figure 1. Molecular structures of $(C_{60};Fc)_{rotax+}$, $(Fc)_{rotax+}$, and Crown-C_{60}.

is a novel fullerene rotaxane that was prepared by utilizing the crown ether−secondary ammonium motif. Related compounds such as $(Fc)_{rotax+}$ and Crown-C_{60} (in Figure 1) were used as reference compounds. The structure of this $(C_{60};Fc)_{rotax+}$ is different from that of the previously reported rotaxane, in which the crown ether is pending on the sidewise position of the C_{60} moiety.[25]

For $(C_{60};Fc)_{rotax+}$, we examined the photoinduced ET and EN processes using time-resolved transient absorption and fluorescence measurements with varying solvent polarity and temperature. The observed results for these photoinduced ET processes of newly synthesized $(C_{60};Fc)_{rotax+}$, in which through-space ET would be anticipated, are compared with the through-bond ET of the covalently connected C_{60}−Fc dyads.[13,26−30] Temperature variation may cause structural changes in the rotaxane with the fluctuation, which would affect the photoinduced events.

Results

Design, Preparation, and Characterization of Rotaxane. The target rotaxane, $(C_{60};Fc)_{rotax+}$, was designed to spatially arrange the C_{60} and Fc moieties in an appropriate distance that is capable of intramolecular ET in the excited state, but not interacting in the ground state. $(C_{60};Fc)_{rotax+}$ can be synthesized by end-capping a pseudorotaxane consisting of a macrocyclic wheel containing a masked diene moiety and a *sec*-ammonium axle with the Fc-group-containing isocyanate via the urethane formation.[31] The end-capping is followed by the introduction of the C_{60} moiety onto the wheel component via the Diels−Alder reaction.[23]

The synthetic route of a crown ether wheel with a masked diene moiety (**6**) and a crown ether wheel with C_{60} moiety (Crown-C_{60}) is outlined in Scheme 1. The monobromination of the sulfur dioxide adduct of 2,3-dimethylbutadiene (**1**) with *N*-bromosuccinimide (NBS) yielded monobrominated sulfolene **2** which was converted to the corresponding azide **3** with sodium azide. Pd-catalyzed hydrogenation of **3** yielded the corresponding amine **4**, which was coupled with acid chloride of crown ether (**5**) to afford **6**. Thermal extrusion of SO_2 and successive Diels−Alder cycloaddition of **6** with C_{60} fullerene afforded Crown-C_{60}.

To realize the above-mentioned strategy, we synthesized a bulky isocyanate, **9**, having a ferrocene moiety as an end-cap, as shown in Scheme 2. Ferrocene was coupled with diazotized 4-nitroaniline, and the resulting nitrophenyl ferrocene **7** was reduced to the corresponding aminophenyl ferrocene **8** by H_2/Pd−C reduction. The reaction of **8** with triphosgene afforded **9**.

According to Scheme 3, a mixture of **10**[32] and a slight excess of **6** was treated with **9** and a tin catalyst to end-cap the terminal hydroxy group of the intermediary pseudorotaxane.[31] Thus, the formed $(Fc)_{rotax+}$ was then converted to C_{60}-tethering rotaxane, $(C_{60};Fc)_{rotax+}$, via the Diels−Alder reaction with C_{60}.[23]

The characterization of these compounds was established on the basis of their fast atom bombardment mass spectrometry (FAB-MS), NMR, IR, and elemental analyses data (see the Experimental Section).

Ground-State Features of $(C_{60};Fc)_{rotax+}$. To examine the ground-state features, cyclic voltammetry and steady-state absorption measurements were performed. In the cyclic voltammetry of $(C_{60};Fc)_{rotax+}$ in deaerated benzonitrile (PhCN) solutions, the first one-electron reduction (E_{red}) and the first one-electron oxidation potentials (E_{ox}) of $(C_{60};Fc)_{rotax+}$ were evaluated to be −0.89 and 0.16 V vs Ag/AgCl, respectively, which correspond to the E_{red} value of Crown-C_{60} (−0.89 V) and the E_{ox} value of $(Fc)_{rotax+}$ (0.15 V) (see the Supporting Information).

The similarity between the E_{red} and E_{ox} values of $(C_{60};Fc)_{rotax+}$ and those of the reference compounds suggests that the electronic interaction among the ferrocene and C_{60} is negligible. The CS state energy levels, which are equivalent to the free-energy changes of CR (ΔG_{CR}), were determined by assessing the difference between the E_{ox} and E_{red} values, correcting the Coulomb energy by the Weller equation.[33] The free-energy changes for CS (ΔG_{CS}) can be calculated by considering the energy levels of the lowest excited states of the C_{60} moiety.[34] The calculated ΔG_{CS} and ΔG_{CR} values are listed in Table 1.

The steady-state absorption spectrum of $(C_{60};Fc)_{rotax+}$ in toluene is virtually a sum of the absorption bands of Crown-C_{60} (at 705 nm, 430 nm, and below 400 nm) and those of $(Fc)_{rotax+}$ (at 440 nm and below 350 nm), as shown in Figure 2. Similar absorption spectra were observed in other solvents. In the present study, the laser excitation of $(C_{60};Fc)_{rotax+}$ and Crown-C_{60} was carried out at 532 nm for transient absorption measurements, and at 410 and 550 nm for fluorescence measurements, which predominantly excite the C_{60} moiety, since Fc does not show substantial absorbance at these wavelengths.

Fluctuation of Optimized Structures. Molecular dynamic (MD) calculations of $(C_{60};Fc)_{rotax+}$ were carried out at various temperatures, since the positions of the C_{60} and Fc moieties may fluctuate within the rotaxane. The MD calculations were performed by the MacroModel package with an MM2 force field and a continuum dielectric constant ($\epsilon = 36.7$ for dimethylformamide (DMF)). Although there is no explicit parameter for $N^+\cdots O$ interactions in the MacroModel method, the calculations may specify the partial charges for the interaction between the N^+ of the axle and the O atoms of the crown ether. Calculated optimized structures change with temperatures. In Figure 3a, the fluctuations of the average center-to-center distances (R_{CC}) between the C_{60} and Fc moieties are plotted with the time at

SCHEME 1: Synthesis of a Macrocycle Containing a C_{60} Moiety (Crown-C_{60})

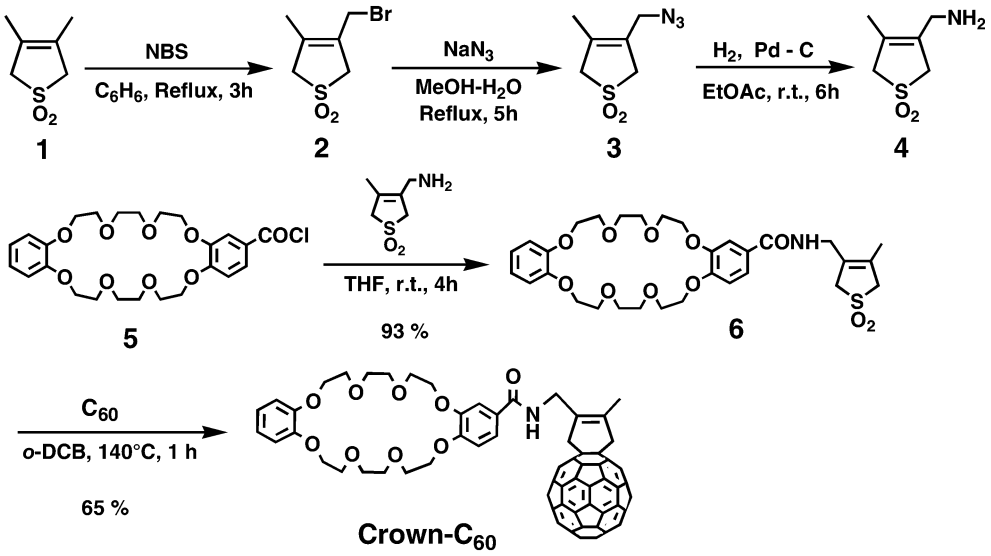

SCHEME 2: Synthesis of a Ferrocene (Fc) End-Cap

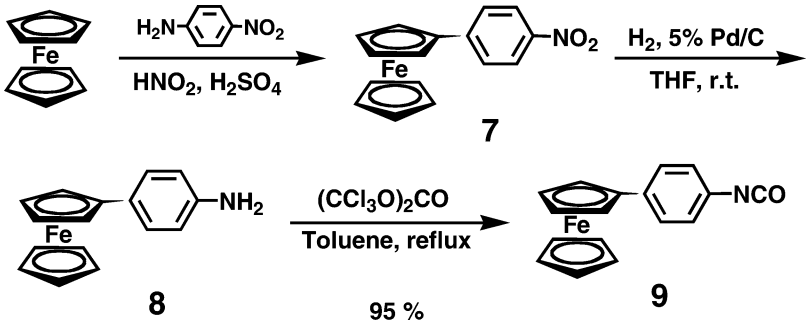

SCHEME 3: Synthesis of Rotaxane $(C_{60};Fc)_{rotax+}$

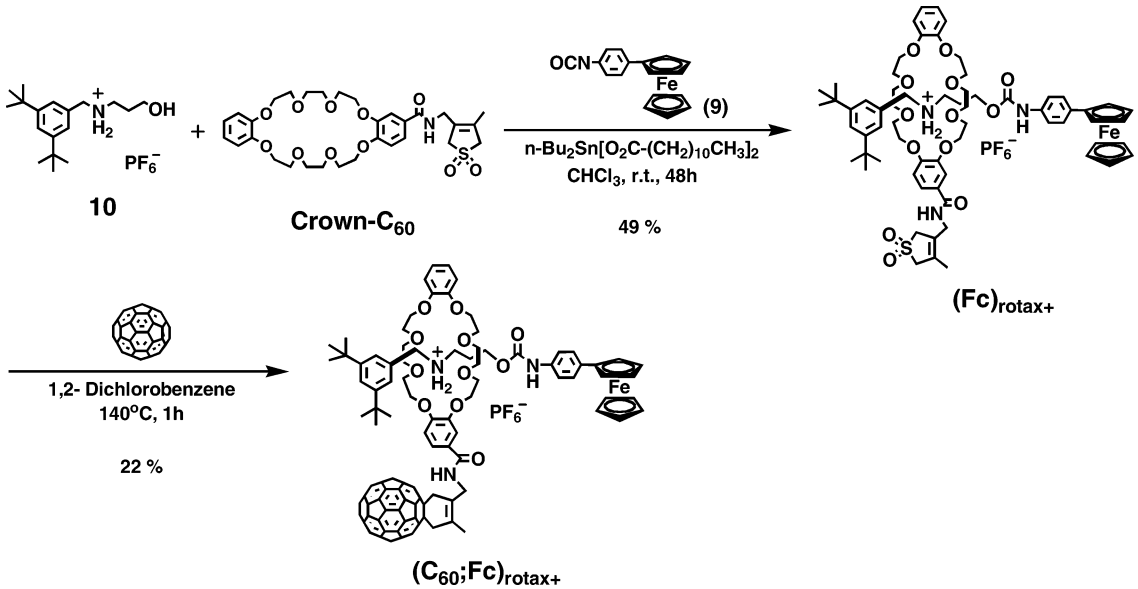

two temperatures; at 270 K, the R_{CC} values fluctuate with an average value of 8 Å, whereas, at 210 K, the fluctuation occurs with an average value of 11 Å. Figure 3b shows the distribution of the R_{CC} values; although the widths of the fluctuations of the R_{CC} values are almost the same for two temperatures, the nearest R_{CC} value at 270 K is shorter than that at 210 K. Typical structures with two R_{CC} values are illustrated in Figure 4a for $R_{CC} = 11$ Å at low temperatures (<230 K) and Figure 4b for $R_{CC} = 8$ Å at high temperatures (>250 K).

Emission Features of $(C_{60};Fc)_{rotax+}$. The steady-state fluorescence spectra of $(C_{60};Fc)_{rotax+}$ and Crown-C_{60} were measured with excitation at 550 nm (Figure 5). The fluorescence peak at 715 nm is attributed to the C_{60} moiety in $(C_{60};Fc)_{rotax+}$. The fluorescence intensity of $(C_{60};Fc)_{rotax+}$ was slightly weaker than that of Crown-C_{60}; the fluorescence intensity in PhCN was almost the same as that in toluene.

The time profiles of the fluorescence intensities at 715 nm $(C_{60};Fc)_{rotax+}$ and Crown-C_{60} in PhCN were measured with a

TABLE 1: Free-Energy Changes for the CS ($-\Delta G_{CS}$) and Free-Energy Changes for the CR ($-\Delta G_{CR}$) of $(C_{60};Fc)_{rotax+}$ at Room Temperature in Various Solvents

solvent	$-\Delta G^{S}_{CS}$[a] (eV)	$-\Delta G^{T}_{CS}$[a] (eV)	$-\Delta G_{CR}$[a] (eV)
toluene	0.12	−0.11	1.63
anisole	0.45	0.22	1.30
THF	0.62	0.39	1.13
PhCN	0.78	0.55	0.97
DMF	0.80	0.58	0.95

[a] $-\Delta G_{CR} = E_{ox} - E_{red} - \Delta G_S$, and $\Delta G^{S,T}_{CS} = E_{0-0}$ ($^1C_{60}$*, $^3C_{60}$*) − ΔG_{CR}; $\Delta E_{0-0} = 1.75$ eV for $^1C_{60}$*, $\Delta E_{0-0} = 1.52$ eV for $^3C_{60}$*, $E_{ox} = 0.16$ V for Fc, and $E_{red} = -0.89$ V for C_{60} vs the Ag/AgCl of $(C_{60};Fc)_{rotax+}$ in PhCN, in which $\Delta G_S = e^2/(4\pi\epsilon_0\epsilon_S R_{CC})$. In other solvents, $\Delta G_S = e^2/(4\pi\epsilon_0)[(1/(2R_+) + 1/(2R_-) - 1/R_{CC})/\epsilon_S - (1/(2R_+) + 1/(2R_-))/\epsilon_R]$, where R_+ and R_- are the radii of the cation and anion, respectively, and R_{CC} is the center-to-center distance of the C_{60} moiety and the Fc moiety; these values were evaluated by the MD calculations. The ϵ_S and ϵ_R are the permittivities of toluene, anisole, THF, PhCN, and DMF, and are 2.38, 4.33, 7.58, 25.20, and 37.00, respectively.

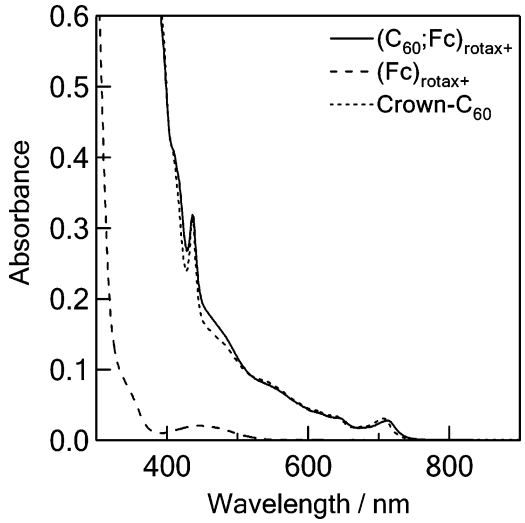

Figure 2. Steady-state absorption spectra of $(C_{60};Fc)_{rotax+}$ (0.1 mM), Crown-C_{60} (0.1 mM), and $(Fc)_{rotax+}$ (0.1 mM) in toluene.

410 nm laser light, as shown in Figure 6; the fluorescence time profile of $(C_{60};Fc)_{rotax+}$ was similar to that of Crown-C_{60} in PhCN. From these time profiles, the fluorescence lifetimes (τ_f) were evaluated by curve-fitting with a single-exponential function, as listed in Table 2.

Time-Resolved Transient Absorption Features of $(C_{60};Fc)_{rotax+}$. Figure 7 shows the time-resolved transient absorption spectrum of $(C_{60};Fc)_{rotax+}$ in toluene observed by the 532 nm laser excitation (6 ns laser pulse) at 298 K. The peak at 700 nm was ascribed to the $^3C_{60}$* moiety in $(C_{60};Fc)_{rotax+}$. The time profile at 700 nm (inset of Figure 7) shows quick decay of the $^3C_{60}$* moiety in the time region until 150 ns, which obeys first-order kinetics, giving a decay rate constant of 2.7×10^7 s^{-1} at 298 K. This decay process may be related to the EN from $^3C_{60}$* to Fc.[35]

As the temperature was lowered to 210 K in toluene, the transient absorption peak appeared at 1000 nm due to the $C_{60}^{\bullet-}$ moiety, in addition to the peak at 720 and 860 nm due to the $^3C_{60}$* moiety, as shown in Figure 8. Since the absorption band of $Fc^{\bullet+}$ was reported to have a small molar absorption coefficient ($\epsilon = 450$ M^{-1} cm^{-1} at $\lambda_{max} = 617$ nm),[36] this band may be hidden under the other huge absorptions. All the decay rates at the absorption peaks slowed at low temperature, including the EN rate from $^3C_{60}$* to Fc. The CR rate of the radical ion pair

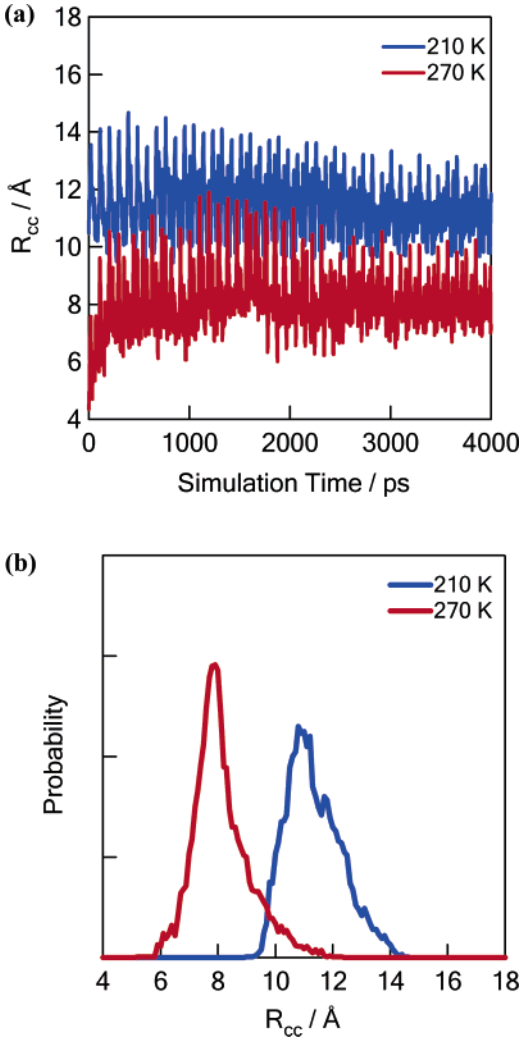

Figure 3. (a) Variation in R_{CC} values as a function of time obtained by MD calculations with an MM2 force field. (b) Distribution of R_{CC} values.

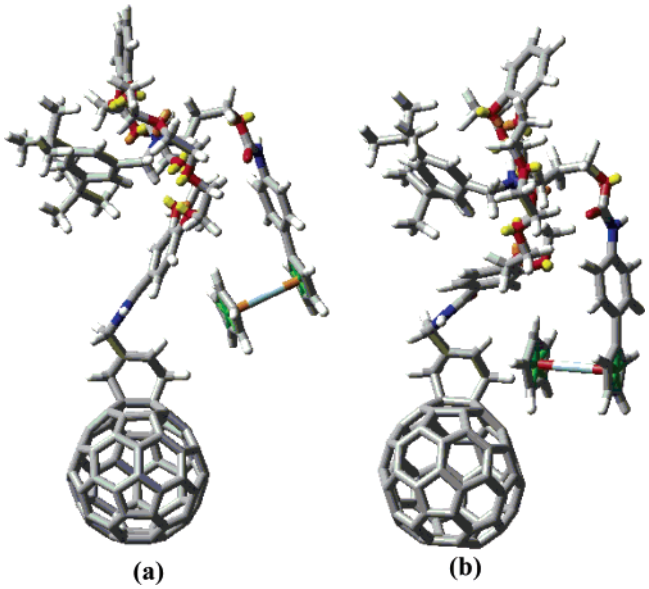

Figure 4. Optimized structures of $(C_{60};Fc)_{rotax+}$ calculated by molecular dynamics: (a) structure with average $R_{CC} = 11$ Å at low temperatures and (b) structure with average $R_{CC} = 8$ Å at high temperatures.

(RIP) was evaluated from the quick decay at 1000 nm at 210 K to be 4.3×10^7 s^{-1}; from the inverse of the k_{CR} value, the

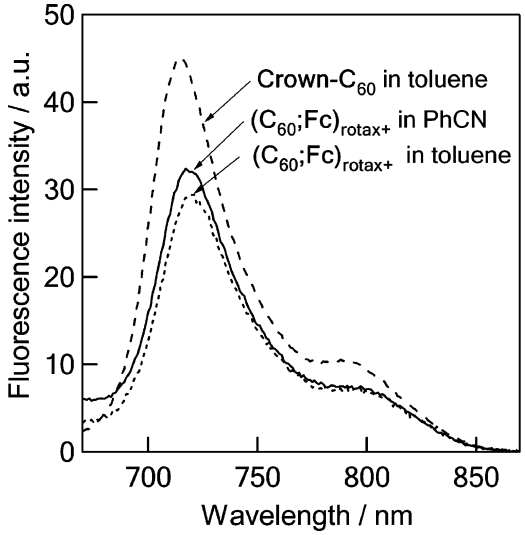

Figure 5. Steady-state fluorescence spectra of $(C_{60};Fc)_{rotax+}$ and Crown-C_{60} (0.1 mM) in PhCN and toluene; $\lambda_{ex} = 550$ nm.

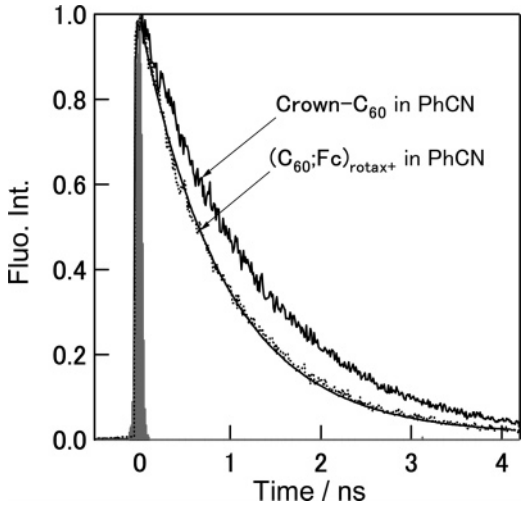

Figure 6. Fluorescence decays of $(C_{60};Fc)_{rotax+}$ and Crown-C_{60} at 715 nm in PhCN at room temperature; $\lambda_{ex} = 410$ nm.

TABLE 2: Fluorescence Lifetimes (τ_f), Rate Constants (k^S_{CS}) and Quantum Yields for CS (Φ^S_{CS}) via $^1C_{60}$* of $(C_{60};Fc)_{rotax+}$ at Room Temperature in Various Solvents

solvent	τ_f (ps)	k^S_{CS}[a] (s^{-1})	Φ^S_{CS}[a]
toluene	920	3.6×10^8	0.33
anisole	940	3.5×10^8	0.32
THF	930	3.5×10^8	0.33
PhCN	980	3.0×10^8	0.29
DMF	950	3.3×10^8	0.31

[a] The lifetimes ($(\tau_f)_{ref}$) of the reference were evaluated to be 1380 ps (Crown-C_{60} in toluene). The k^S_{CS} and Φ^S_{CS} were calculated from $k^S_{CS} = (1/\tau_f)_{sample} - (1/\tau_f)_{ref}$ and $\Phi^S_{CS} = [(1/\tau_f)_{sample} - (1/\tau_f)_{ref}]/(1/\tau_f)_{sample}$.

lifetime of the RIP (τ_{RIP}) was evaluated to be 23 ns. Similar trends were also observed in less polar solvents such as anisole and tetrahydrofuran (THF). The τ_{RIP} values of $(C_{60}^{\bullet-};Fc^{\bullet+})_{rotax+}$ are 40 ns (at 235 K) in anisole and 143 ns (at 210 K) in THF, as listed in Table 3.

In the transient spectrum of $(C_{60};Fc)_{rotax+}$ in DMF observed at room temperature (Figure 9), a transient absorption band of the $C_{60}^{\bullet-}$ moiety clearly appeared at 1000 nm, indicating the generation of $(C_{60}^{\bullet-};Fc^{\bullet+})_{rotax+}$. Similar transient absorption spectra suggesting the formation of $(C_{60}^{\bullet-};Fc^{\bullet+})_{rotax+}$ were obtained in PhCN (see the Supporting Information). The τ_{RIP}

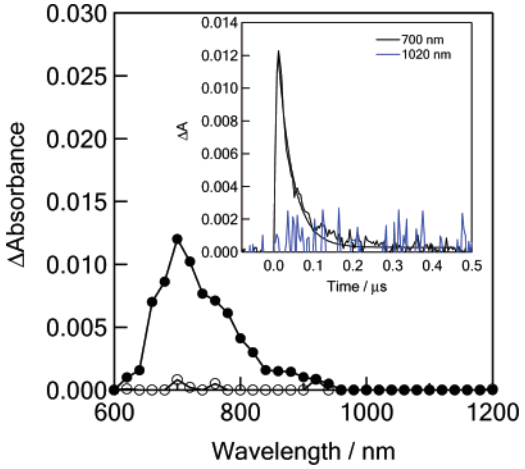

Figure 7. Nanosecond transient absorption spectra of $(C_{60};Fc)_{rotax+}$ (0.1mM) in toluene observed by 532 nm laser irradiation at 16 ns (●) and 400 ns (○) at 298 K. Inset: Absorption−time profiles.

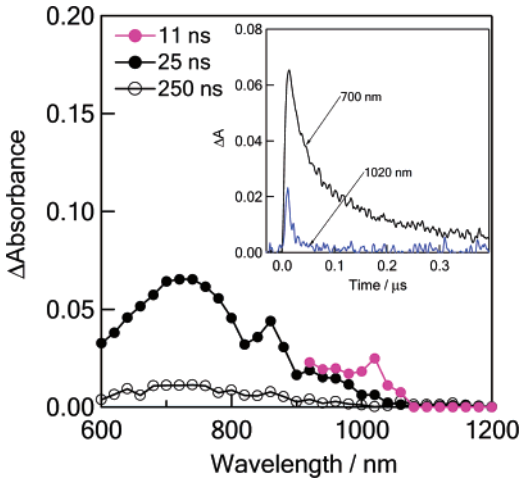

Figure 8. Nanosecond transient absorption spectra of 0.2 mM $(C_{60};Fc)_{rotax+}$ in toluene at 253 K, observed by 532 nm laser irradiation at 11 ns (fuchsia circles), 25 ns (black circles), and 250 ns (open circles). Inset: Absorption−time profiles.

TABLE 3: Energy-Transfer Rate Constants of $^3C_{60}$* (k^T_{EN}), CR Rate Constants (k_{CR}), and Lifetimes (τ_{RIP}) of $(C_{60}^{\bullet-};Fc^{\bullet+})_{rotax+}$ in Various Solvents

solvent	temperature (K)	k^T_{EN}[a] (s^{-1})	k_{CR}[b] (s^{-1})	τ_{RIP} (ns)
toluene	300	2.7×10^7		
	210	1.9×10^7	4.3×10^7	23
anisole	300	3.2×10^7		
	235	2.0×10^7	2.5×10^7	40
THF	300	2.9×10^7		
	210	5.8×10^6	7.0×10^6	143
PhCN	300	5.5×10^7	3.0×10^7	33
	260	1.8×10^7	2.4×10^7	42
DMF	300	7.7×10^7	5.1×10^7	20
	210	2.5×10^6	3.8×10^6	263

[a] From the decay of $^3C_{60}$* at 700 nm. [b] From the decay of $C_{60}^{\bullet-}$ at 1000 nm.

values of $(C_{60}^{\bullet-};Fc^{\bullet+})_{rotax+}$ were evaluated to be 20 and 33 ns in DMF and PhCN, respectively, at room temperature (298 K).

As the temperature was lowered to 208 K in DMF, the transient absorption spectra became similar to that of the $^3C_{60}$* moiety, as shown in Figure 10, in which the absorption of the $C_{60}^{\bullet-}$ moiety remained at 1000 nm. Similar transient absorption spectra were observed upon lowering the temperature in PhCN (see the Supporting Information).

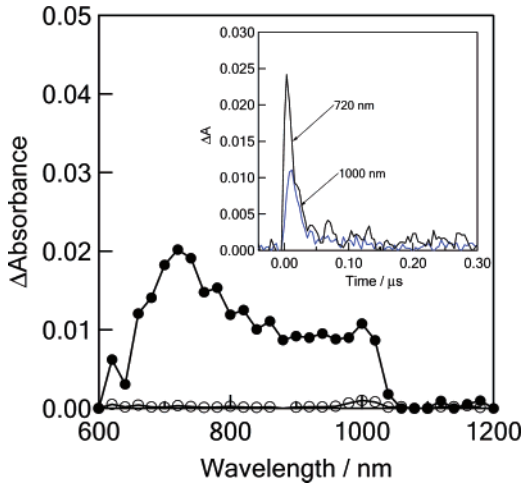

Figure 9. Nanosecond transient absorption spectra of $(C_{60};Fc)_{rotax+}$ (0.1mM) observed by 532 nm laser irradiation at 8 ns (●) and 300 ns (○) in DMF at 298 K. Inset: Absorption−time profiles.

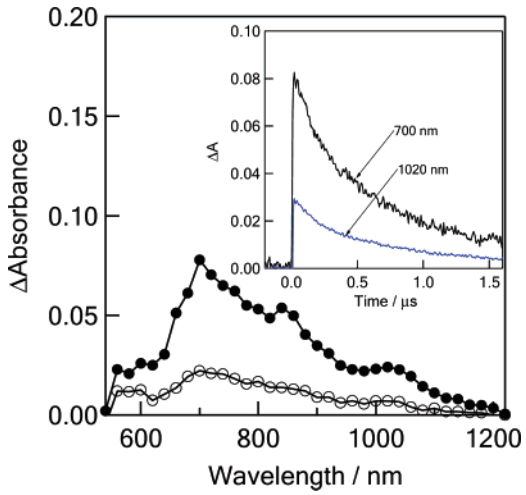

Figure 10. Nanosecond transient absorption spectra of $(C_{60};Fc)_{rotax+}$ (0.2 mM) observed by 532 nm laser irradiation at 0.1 μs (●) and 1 μs (○) in DMF at 208 K. Inset: Absorption−time profiles.

Discussion

The ΔG_{CS} values via $^1C_{60}$* and via $^3C_{60}$* in PhCN were evaluated to be −0.78 and −0.55 eV, respectively (Table 1); thus, both CS processes are exothermic. In DMF, more exothermic CS processes would be anticipated, whereas the CS processes become less exothermic in THF and anisole. In toluene, the CS process via the $^3C_{60}$* moiety becomes endothermic.

The steady-state absorption and electrochemical studies of $(C_{60};Fc)_{rotax+}$ indicate that there is no significant interaction between the C_{60} and Fc moieties in the ground state.

The MD calculations of $(C_{60};Fc)_{rotax+}$ revealed that optimized structures have penetrating interlocked structures, as shown in Figure 4. These optimized structures may be determined by many factors such as $\pi-\pi$ interaction, van der Waals force, static Coulomb force, and so forth. Although there is no explicit parameter for the $N^+\cdots O$ interaction between the axle and the wheel in the MacroModel (MM2) calculations, the resultant partial atomic charges between the N^+ and O atoms may work to keep the rotaxane structures, as shown in Figure 4. At 210 K, the R_{CC} values fluctuate between 9.5 and 14.5 Å, keeping the average R_{CC} values at 11 Å with an interval of ∼100 ps, due to the movement of Fc and C_{60} accompanied by the rotation and stretching of bonds in the rotaxane skeleton (Figure 3). From 210 to 270 K, a considerable decrease in the fluctuation range was observed from 6 to 12 Å, keeping the average R_{CC} values at 8 Å. With further rising temperature up to 330 K, the R_{CC} values fluctuate between 6 and 16 Å. The minimum R_{CC} value may be important for the ET and EN processes; between 270 and 330 K, the minimum R_{CC} value was 6 Å, whereas, at 210 K, this value increased to 9.5 Å.

From the steady-state fluorescence studies, the relative fluorescence intensities of $(C_{60};Fc)_{rotax+}$ in toluene and PhCN were slightly weaker than that of Crown-C_{60}, suggesting a weak quenching of the singlet excited state of the C_{60} moiety ($^1C_{60}$*) by the Fc of $(C_{60};Fc)_{rotax+}$ in both solvents. Furthermore, the time-resolved fluorescence studies of $(C_{60};Fc)_{rotax+}$ in both polar and nonpolar solvents indicate that the τ_f values of $(C_{60};Fc)_{rotax+}$ were nearly equal in the 900−1000 ps region, which are only slightly shorter than that of Crown-C_{60} (1380 ps).[37] From the negative ΔG^S_{CS} values of $(C_{60};Fc)_{rotax+}$ in solvents including toluene, the CS process via the $^1C_{60}$* moiety in $(C_{60};Fc)_{rotax+}$ is thermodynamically favorable; thus, the shorter τ_f values of $(C_{60};Fc)_{rotax+}$ compared to those of Crown-C_{60} can be attributed to the CS process via the $^1C_{60}$* moiety. The rate constant (k^S_{CS}) and the quantum yield (Φ^S_{CS}) for the CS process via the $^1C_{60}$* moiety of $(C_{60};Fc)_{rotax+}$ were calculated as $(3-4) \times 10^8$ s^{-1} and 0.30−0.35, respectively, as listed in Table 2. These small values are characteristic of rotaxanes, since we found that the CS process via the $^1C_{60}$* moiety is minor for the rotaxanes of $(C_{60};amine)_{rotax}$.[38]

From the nanosecond transient absorption studies of $(C_{60};Fc)_{rotax+}$ in toluene, the fast quenching rate constant of the $^3C_{60}$* moiety can be attributed to the EN process from the $^3C_{60}$* moiety to the Fc moiety;[35] thus, the decay rate of the $^3C_{60}$* moiety can be attributed to the rate of the EN process (k^T_{EN} in Table 2). The absorption of the $C_{60}^{\bullet-}$ moiety, which is expected to appear at 1000 nm, was not observed in toluene at 298 K, suggesting that $(C_{60}^{\bullet-};Fc^{\bullet+})_{rotax+}$ produced via $^1C_{60}$* with low Φ^S_{CS} values (Table 1) is short-lived and not persistent in a time region longer than 6 ns (inset of Figure 7). Interestingly, when the temperature was lowered to 210 K in toluene, all the decay rates at the absorption peaks slowed, including the EN rate from $^3C_{60}$* to Fc, suggesting a decrease in the k^T_{EN} values, which may be related to the fluctuated structural changes of $(^3C_{60}*;Fc)_{rotax+}$ similar to those in the ground state, as shown in Figure 3.

The τ_{RIP} value of $(C_{60}^{\bullet-};Fc^{\bullet+})_{rotax+}$ was evaluated to be 23 ns at 210 K in toluene. The τ_{RIP} values of $(C_{60}^{\bullet-};Fc^{\bullet+})_{rotax+}$ in anisole (40 ns) and THF (143 ns) are longer than those in toluene, although they are quite shorter than those in DMF (270 ns) at 210 K. As an origin of the observed prolongation of $(C_{60}^{\bullet-};Fc^{\bullet+})_{rotax+}$ in polar solvents, one can consider that the CS process occurs via the $^3C_{60}$* moiety as expected from the sufficiently negative $\Delta G_{CS}{}^T$ values, affording $(C_{60}^{\bullet-};Fc^{\bullet+})_{rotax+}$ with triplet spin character, which may be in equilibrium with $(^3C_{60}*;Fc)_{rotax+}$. This equilibrium could be confirmed by the faster decay rates of the $^3C_{60}$* moiety in highly polar solvents compared to those in less polar solvents (compare the 700 nm decay in Figure 7 with that in Figure 9). Thermodynamically, the CS process via ^3Fc* is possible in DMF and PhCN after the EN process via $^3C_{60}$*.

The k_{CR} values of $(C_{60}^{\bullet-};Fc^{\bullet+})_{rotax+}$ evaluated by the initial fast decay part showed temperature dependence. According to the semiclassical Marcus equation,[39] the ET rate constant (k_{ET}) can be described as follows (eq 1):

$$\ln(k_{ET}T^{1/2}) = \ln\{2\pi^{3/2}|V|^2/[h(\lambda k_B)^{1/2}]\} - \Delta G^{\neq}/(k_BT) \quad (1)$$

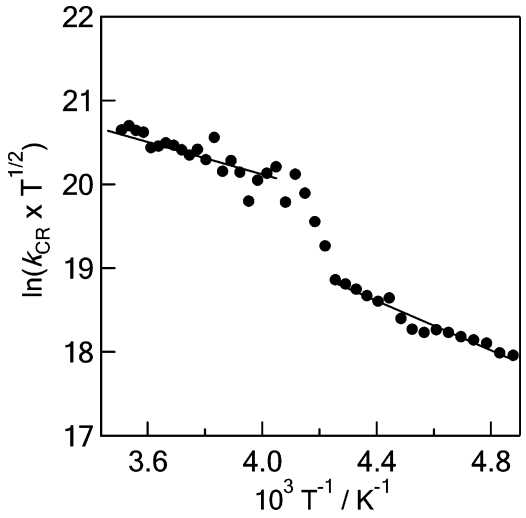

Figure 11. Semiclassical Marcus (modified Arrhenius) plots of k_{CR} for $(C_{60};Fc)_{rotax+}$ in DMF.

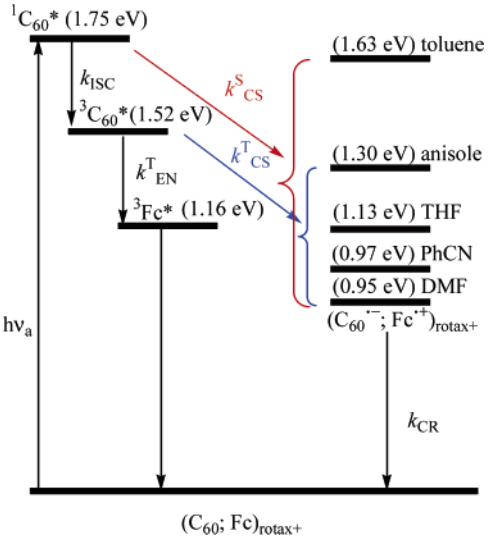

Figure 12. Schematic energy diagram for the electron-transfer processes of $(C_{60};Fc)_{rotax+}$ in toluene, anisole, THF, PhCN, and DMF.

where T, h, and k_B refer to the absolute temperature, Planck constant, and Boltzmann constant, respectively; $|V|$, λ, and $\Delta G^{\ddagger}$ refer to the electron coupling matrix element, the reorganization energy, and the Gibbs activation energy in the Marcus theory, respectively.[39] Plots of $\ln(k_{CR} \times T^{1/2})$ in DMF against $1/T$ for $(C_{60}^{\bullet-};Fc^{\bullet+})_{rotax+}$ are shown in Figure 11, in which two straight lines are obtained; one is in the 290−250 K region with $\Delta G^{\neq} = 0.080$ eV, while another is in the 235−207 K region with $\Delta G^{\neq} = 0.126$ eV for the CR process of $(C_{60}^{\bullet-};Fc^{\bullet+})_{rotax+}$.

These $\Delta G^{\neq}$ values are slightly smaller than those for covalently bonded dyad systems such as retinyl−C_{60} (0.16 eV).[40] Such small $\Delta G^{\neq}$ values are characteristic of rotaxane, in which the through-space ET takes place.[23a] Furthermore, the $\Delta G^{\neq}$ value for the CR process of $(C_{60}^{\bullet-};Fc^{\bullet+})_{rotax+}$ in the higher temperature region is smaller than that in the lower temperature region, reflecting the easy fluctuation of the rotaxane in higher temperature, which was experimentally suggested by the broadening of the signals of ^{1}H NMR (see Supporting Information). A critical change in the drastic change in fluctuation seems to exist in the 235−250 K region, which was supported by the MD calculations (Figure 3).

In the high-temperature region, the short minimum distance between the $C_{60}^{\bullet-}$ moiety and the $Fc^{\bullet+}$ moiety in the fluctuating structures promotes the k_{CR} value of $(C_{60}^{\bullet-};Fc^{\bullet+})_{rotax+}$, whereas, in the low-temperature region, the long minimum distance during the fluctuation of $(C_{60}^{\bullet-};Fc^{\bullet+})_{rotax+}$ decreases the encounter frequency to retard the CR rate.

Energy Diagram for Solvent Effect on Photoinduced ET. From the ΔG_{CR}, ΔG^S_{CS}, and ΔG^T_{CS} values, as well as the energy levels of the lowest excited singlet states, an energy diagram for $(C_{60};Fc)_{rotax+}$ can be illustrated, as shown in Figure 12. In toluene, the CS process via $^1C_{60}$* is possible, but the lifetime of $(C_{60}^{\bullet-};Fc^{\bullet+})_{rotax+}$ is very short because an efficient CR process to the $^3C_{60}$* level or to the ground state is possible. In anisole and THF, since the energy levels of the CS states are lower than those of $^1C_{60}$* and $^3C_{60}$*, the CS processes via $^1C_{60}$* and $^3C_{60}$* are possible; however, the CS process via $^3C_{60}$* may be less effective because the energy differences are small. Therefore, the CS process via $^1C_{60}$* predominantly yields the singlet spin-state of $(C_{60}^{\bullet-};Fc^{\bullet+})_{rotax+}$ with a short lifetime. In polar solvents such as DMF and PhCN, since the energy levels of the CS state are lower than those of $^1C_{60}$*, $^3C_{60}$*, and ^{3}Fc*, the CS processes via $^1C_{60}$*, $^3C_{60}$*, and ^{3}Fc* are all possible. Slow CR rates may be related to the triplet spin character of $(C_{60}^{\bullet-};Fc^{\bullet+})_{rotax+}$.

Comparison with Other Rotaxanes. Compared with rotaxanes with C_{60} and porphyrin moieties[23] and phthalocyanine moieties,[22] in which the CS process takes place mainly via the excited states of the porphyrin and phthalocyanine, the CS process of $(C_{60};Fc)_{rotax+}$ takes place via the excite states of the C_{60} moiety similar to $(C_{60}$:amine$)_{rotax}$.[38] For the CS process of rotaxanes composed of the C_{60} and zinc porphyrin moiety, contribution of the CS process via the excited singlet state of the zinc porphyrin moiety tends to increase for the short axle because of a decrease in the fluctuation.[23] For $(C_{60};Fc)_{rotax+}$, the contribution of the $^3C_{60}$* moiety to the CS process may be predominant because of the short axle length with relatively small fluctuation. In the case of rotaxanes composed of zinc porphyrin as an electron donor and Au^+ porphyrins as an electron acceptor, a superexchange mechanism was confirmed.[41] However, for $(C_{60};Fc)_{rotax+}$, any clear evidence showing the superexchange mechanism may not be obtained because of the smaller π-systems of the Fc moiety and the spherical C_{60} moiety.

$(C_{60}^{\bullet-};Fc^{\bullet+})_{rotax+}$ has shorter τ_{RIP} values compared with those of different types of rotaxanes bearing C_{60} and porphyrin, which have the τ_{RIP} value of 180−900 ns in PhCN at room temperature.[23] Compared with the τ_{RIP} values of $(C_{60}$;amines$)_{rotax+}$ longer than 200 ns at room temperature, in which the CS process predominantly takes place via $^3C_{60}$*,[38] the τ_{RIP} values of $(C_{60};Fc)_{rotax+}$ at room temperature are quite shorter, probably due to small ΔG_{CR} values similar to the reorganization energy,[15b,c] leading to near the top region of the Marcus parabola.[39] Furthermore, the τ_{RIP} values of $(C_{60};Fc)_{rotax+}$ were longer than the previously reported ones for a quite different structure of rotaxane,[25] in which the τ_{RIP} value is 10−13 ns in DMF and PhCN, at room temperature.

Conclusions

In $(C_{60};Fc)_{rotax+}$, the photoinduced CS process takes place both via the $^1C_{60}$* moiety and via the $^3C_{60}$* moiety, producing $(C_{60}^{\bullet-};Fc^{\bullet+})_{rotax+}$ with lifetimes of 20−33 ns in DMF and PhCN at room temperature. For $(C_{60}^{\bullet-};Fc^{\bullet+})_{rotax+}$, the through-space CR process was presumed from the low activation free energies, as evaluated experimentally by the temperature dependence of the rate constants for the CR process. It is also revealed that the fluctuation of the distance between the C_{60} moiety and the

Fc moiety in $(C_{60};Fc)_{rotax+}$ is important to control the CR process in rotaxane. Thus, at low temperatures, longer lifetimes of $(C_{60}^{\bullet-};Fc^{\bullet+})_{rotax+}$ were observed in polar and nonpolar solvents, affording wide applications to artificial photosynthetic systems.

Experimental Section

General Methods. Melting points were measured on a Yanagimoto micro melting point apparatus and a Stuart Scientific melting point apparatus and were uncorrected. IR spectra were recorded on a JASCO FT-IR model 230 spectrometer. ^{1}H NMR spectra were recorded on a JEOL JNM-GX-270, a JNM-L-400, and a JNM-GX-500 spectrometer. FAB-MS measurements were performed on a Finnigan TSQ-70 instrument. For preparative high-performance liquid chromatography (HPLC), a JAICO LC-908 system equipped with columns JAIGEL-1(∅20 × 600 mm) and JAIGEL-2 (∅20 × 600 mm) was used. Compounds **1** [23] and **5** were synthesized by the reported methods.

Synthesis of Crown-C_{60}. *Preparation of **2**.* A mixture of **1** (1.5 g, 10.27 mmol), NBS (2.1 g, 11.81 mmol) and benzoyl peroxide (200 mg, 0.83 mmol) in benzene (40 mL) was refluxed under Ar atmosphere for 3 h. The mixture was filtered. The crude product obtained after the removal of the solvent in vacuo was subjected to column chromatography over silica gel. The chromatographic separation (eluent: ethyl acetate/hexane = 20:80) afforded **2** (1.15 g, 50%), which was used for the next step in the reaction without further purification. ^{1}H NMR ($CDCl_3$, 270 MHz): δ 4.03 (s, 2H, CH_2Br), 3.85 (s, 2H, CH_2), 3.74 (s, 2H, CH_2), 1.82 (s, 2H, CH_3).

*Preparation of **3**.* To a solution of NaN_3 (886 mg, 13.6 mmol) in MeOH−H_2O (2:1 v/v, 30 mL) was added **2** (1.02 g, 4.54 mmol), and the mixture was refluxed for 5 h. The reaction mixture was poured into water and extracted with chloroform (3 × 50 mL). The chloroform layer was dried over anhydrous $MgSO_4$, filtered, and evaporated in vacuo to give the crude product. Column chromatography over silica gel (eluent: 30% ethyl acetate in hexane) gave **3** as a colorless oil (757 mg, 89.0%). ^{1}H NMR ($CDCl_3$, 270 MHz): δ 3.98 (s, 2H, CH_2N_3), 3.82 (s, 2H, CH_2), 3.78 (s, 2H, CH_2), 1.87 (s, 2H, CH_3); IR ($CDCl_3$) cm^{-1}: 2101 (N_3).

*Preparation of **4**.* To a suspension of 10% Pd−C (80 mg) in ethyl acetate (40 mL) was added **3** (710 mg, 3.79 mmol), and the mixture was stirred for 6 h at room temperature under hydrogen atmosphere. Pd−C was removed by filtration, and the solvent was evaporated. Column chromatography of the residual product over silica gel (eluent: 10% MeOH in $CHCl_3$) gave **4** as a colorless oil (329 mg, 54.0%). ^{1}H NMR ($CDCl_3$, 270 MHz): δ 3.85 (s, 2H, CH_2), 3.72 (s, 2H, CH_2), 3.42 (s, 2H, CH_2), 1.78 (s, 2H, CH_3), 1.3 (bs, NH_2).

*Preparation of **6**.* To a solution of **4** (295 mg, 1.83 mmol) and Et_3N (557 mg, 5.50 mmol) in THF (10 mL), a solution of acid chloride of crown ether (**5**; 920 mg, 1.80 mmol) in THF (50 mL) was added at 0°C. The reaction mixture was stirred at 0 °C for 1 h and at room temperature for 4 h. The reaction mixture was diluted with 200 mL $CHCl_3$ and washed with 1M HCl (75 mL) and water (75 mL). Evaporation of the solvent gave the crude product, which was chromatographed over silica gel (eluent: 10% MeOH/EA) to give **6** as a white solid (1.07 g, 93%). ^{1}H NMR ($CDCl_3$, 270 MHz): δ 7.28 (m, 1H, Ar−H), 7.2 (m, 1H, Ar−H), 6.79−6.83 (m, 5H, Ar−H), 6.32 (bs, 1H, −NH), 3.68−4.11 (m, 30H, CH_2 of DB24C8 and sulfolene), 1.97 (s, 3H, CH_3).

Preparation of Crown-C_{60}. A mixture of **6** (50 mg, 0.04 mmol) and fullerene (122 mg, 0.17 mmol) in 1,2-dichlorobenzene (30 mL) was heated at 140 °C for 1 h. The reaction mixture was passed through a short column of silica gel. Toluene eluted first the unreacted fullerene, and the MeOH−$CHCl_3$ mixed solvent (1/10, v/v) eluted the crude product, which was purified by HPLC to afford Crown-C_{60} (32 mg, 42%).

Synthesis of Ferrocene−Isocyanate 9. *Preparation of **7**.* Ferrocene (12.5 g, 67 mmol) was added to 95% sulfuric acid (70 mL) with stirring. The temperature was slowly raised to 50 °C, and a blue solution of $[Fe(C_5H_5)_2]^+$ appeared. The resulting solution was kept at room temperature overnight and then poured into ice water. 4-Nitroaniline (8.6 g, 62 mmol) was diazotized with 4.3 g (62 mmol) of $NaNO_2$ and excess hydrochloric acid, and the mixture was added to the blue solution at room temperature. The reaction mixture was vigorously stirred by a mechanical stirrer for 24 h. The reaction mixture was filtered, and the brown precipitate formed from the filtrate was extracted with $CHCl_3$ (200 mL). Removal of the solvent in vacuo afforded the crude product, which was chromatographed over alumina (eluent: $CHCl_3$/Hexane = 1:1) to afford **7** (1.8 g, 9%). ^{1}H NMR ($CDCl_3$, 270 MHz): δ 8.04 (d, 2H, Ar−H, J = 8 Hz), 7.46 (d, 2H, Ar−H, J = 8 Hz), 4.64 (s, 2H, −CH═), 4.39(s, 2H, −CH═), 3.98 (s, 5H, −CH═); mp 174.6−175.2 °C.

*Preparation of **8**.* Compound **7** (1.2 g, 3.9 mmol) was stirred with 5% Pd/C (450 mg) in THF (50 mL) under H_2 atmosphere at room temperature for 6 h during which the color of the mixture changed to orange. The reaction mixture was filtered, and the filtrate was evaporated. The residual product was purified by column chromatography over silica gel to give the amine **8** as an orange solid (0.70 g, 65%) ^{1}H NMR ($CDCl_3$, 270 MHz): δ 7.21 (d, 2H, Ar−H, J = 1.9 Hz), 6.55 (d, 2H, Ar−H, J = 1.9 Hz), 4.44 (s, 2H, −CH═), 4.14 (s, 2H, −CH═), 3.94 (s, 5H, −CH═), 3.52 (bs, 2H, NH_2), mp 157.4−158 °C.

*Preparation of **9**.* To a solution of **8** (355 mg, 1.28 mmol) in toluene (30 mL), dry gaseous HCl was bubbled for 10 min until the hydrochloride salt was precipitated. To the resulting mixture, triphosgene (760 mg, 2.56 mmol) was added, and the mixture was refluxed for 2 h. Removal of the solvent in vacuo from the reaction mixture afforded the isocyanate **9** (370 mg, 95%). ^{1}H NMR ($CDCl_3$, 270 MHz): δ 7.35 (d, 2H, Ar−H, J = 7.6 Hz), 6.98 (d, 2H, Ar−H, J = 7.8 Hz), 4.65 (s, 2H, −CH═), 4.37 (s, 2H, −CH═), 4.07 (s, 5H, −CH═); IR (KBr) cm^{-1}: 2263 (s); FAB-MS (m/z): 303 (M^+); Calcd for $C_{91}H_{41}NO_9$ $(H_2O)_{0.5}$: C, 65.40; H, 4.52; N, 4.48; Found: C, 64.98; H, 4.50; N, 4.10; mp 106.3−107.4 °C.

Synthesis of $(Fc)_{rotax+}$. To a mixture of the axle (**10**;[32] 43 mg, 0.1 mmol) and DB24C8 having a sulfolene unit (**6**, 76 mg, 0.12 mmol) in chloroform (0.6 mL) were added **9** (61 mg, 0.20 mmol) and di-*n*-butyltin dilaurate (DBTDL) (12 μL, 0.02 mmol). The mixture was stirred at room temperature for 48 h under Ar atmosphere. After the removal of solvent, the residual mixture was subjected to HPLC separation to give rotaxane ($(Fc)_{rotax+}$) (67 mg, 49%). ^{1}H NMR ($CDCl_3$, 270 MHz): δ 7.58 (m, 2H, Ar−H of end-cap), 7.44 (bs, 1H, −NH), 7.36−7.28 (m, 8H, Ar−H of end-cap, axle, and wheel), 6.93−6.88 (m, 4H, Ar−H of wheel), 6.85 (bs, 1H, −NH), 4.6−3.24 (m, 45H, CH_2 of axle and wheel, CH═ of end-cap), 1.91 (s, 3H, CH_3 of wheel), 1.78 (bs, 2H, CH_2 of axle), 1.20 (s, 18H, *tert*-butyl of axle); ^{13}C NMR ($CDCl_3$, 100 MHz): δ 166.86, 153.34, 151.44, 150.00, 147.36, 147.04, 136.16, 134.02, 131.50, 128.61, 127.59, 127.37, 126.48, 124.15, 123.22, 122.24, 122.04, 121.94,118.80, 113.02, 112.84, 112.00, 111.92, 77.25, 77.04, 76.73, 70.62, 70.52, 70.24, 70.10, 69.91, 69.72, 69.06, 68.70, 68.25, 66.29, 61.19, 60.96, 58.30, 52.87, 46.20, 37.52, 37.20, 34.80, 31.35, 26.23, 14.73; FAB-

MS (*m*/*z*): 1218.2 [M − PF_6 + H]$^+$, 20%, 1152.6 [(M − PF_6 + H) − SO_2]$^+$, 100%; IR (KBr) cm^{-1}: 3404 (N−H), 3166 (N−H), 1719 (O−CO−NH), 1654 (CO−NH), 1311 (S═O_{asymm}), 1106 (S═O_{symm}), 843(P−F_{symm}); Calcd for $C_{66}H_{86}F_6FeN_3O_{13}PS$ $(H_2O)_{1.0}$: C, 58.19; H, 6.36; N, 3.08; Found: C, 57.43; H, 6.43; N, 3.04; mp 132−134 °C (decomp).

Synthesis of $(C_{60};Fc)_{rotax+}$. A mixture of $(Fc)_{rotax+}$ (50 mg, 0.037 mmol) and fullerene (107 mg, 0.15 mmol) in 1,2-dichlorobenzene (5 mL) was heated at 140 °C for 1 h. The mixture was passed through a short column of SiO_2 (solvent: 1−5% MeOH in $CHCl_3$) to give the crude product, which was purified by HPLC to afford $(C_{60};Fc)_{rotax+}$ (22 mg, 22%) as a brownish-red film. ^{1}H NMR ($CDCl_3$, 270 MHz): δ 7.8 (m, 2H, Ar−H of end-cap), 7.62 (bs, 1H, −NH), 7.5−7.36 (m, 8H, Ar−H of end-cap, axle, and wheel), 6.91−6.89 (m, 4H, Ar−H of wheel), 6.81 (bs, 1H, −NH), 4.58−3.32 (m, 45H, CH_2 of axle and wheel, CH═ of end-cap), 2.44 (s, 3H, CH_3 of wheel), 1.75 (bs, 2H, CH_2 of axle), 1.21 (s, 18H, *tert*-butyl of axle) at 298 K (for ^{1}H NMR at 333 K, see Supporting Information). ^{13}CNMR ($CDCl_3$, 100 MHz): δ 166.78, 157.38, 157.14, 153.44, 149.68, 147.59, 147.50, 147.45, 147.38, 146.34, 146.16, 146.08, 145.98, 145.88, 145.74, 145.06, 144.72, 142.94, 142.35, 142.05, 141.98, 141.61, 141.42, 141.42, 141.37, 140.04, 139.86, 136.31, 135.94, 135.76, 133.81, 132.29, 131.65, 128.31, 123.32, 122.11, 121.94, 118.91, 113.02, 112.97, 112.55, 112.09, 104.35, 102.2, 85.40, 77.61, 70.29, 70.16, 70.06, 69.93, 69.77, 69.03, 68.33, 66.51, 66.28, 61.01, 56.47, 52.77, 46.94, 46.22, 42.80, 40.61, 29.70, 26.23, 19.66; FAB-MS (*m*/*z*): 1874 [M − PF_6]$^+$; IR (KBr) cm^{-1}: 3423 (N−H), 3166 (N−H), 1719 (O−CO−NH), 1654 (CO−NH), 842 (P−F_{symm}); Calcd for $(C_{126}H_{86}F_6FeN_3O_{11}P)$-$(CHCl_3)(C_6H_{14})(H_2O)$: C, 71.81; H, 4.58; N, 1.89; Found: C, 71.20; H, 4.25; N, 1.47.

Spectral Measurements. The time-resolved fluorescence spectra were measured by the single-photon counting method using the second harmonic generation (SHG, 410 nm) of a Ti: sapphire laser [Spectra-physics, Tsunami 3950-L2S, full width at half-maximum (fwhm) = 1.5 ps] and a streak scope (Hamamatsu Photonics, C4334−01) equipped with a polychromator as the excitation source and detector, respectively.

Nanosecond transient absorption measurements were carried out using the SHG (532 nm) of a Nd:YAG laser (Spectra Physics, Quanta-Ray GCR-130, fwhm = 6 ns) as the excitation source. For the transient absorption spectra in the near-IR region (600−1600 nm), the monitoring light from a pulsed Xe lamp was detected with a Ge-avalanche photodiode (Hamamatsu Photonics, B2834). The details of the transient absorption measurements were described elsewhere.[42] All the samples in a quartz cell (1 × 1 cm) were deaerated by bubbling argon through the solution for 15 min.

Electrochemical Measurements. The cyclic voltammetry measurements were performed on a BAS CV-50 W electrochemical analyzer in a deaerated benzonitrile solution containing 0.10 M Bu_4NPF_6 as a supporting electrolyte at 298 K (100 mV s^{-1}). The glassy carbon working electrode was polished with a BAS polishing alumina suspension and rinsed with acetone before use. The counter electrode was a platinum wire. The measured potentials were recorded using a Ag/AgCl (saturated KCl) electrode as the reference electrode.

Acknowledgment. The present work was partly supported by a Grant-in-Aid for Scientific Research primary area (417) from the Japan Society for the Promotion of Science and the Ministry of Education, Science, Sports and Culture of Japan.

Supporting Information Available: Cyclic voltammograms for $(C_{60};Fc)_{rotax+}$. Transient absorption spectra and time profiles of Crown-C_{60} in toluene, and $(C_{60};Fc)_{rotax+}$ in anisole, THF, and PhCN (at room temperature and low temperatures). ^{1}H NMR spectra of $(C_{60};Fc)_{rotax+}$ at 298 and 333 K. This material is available free of charge via the Internet at http://pubs.acs.org.

References and Notes

(1) Balzani, V.; Scandola, F. *Supramolecular Photochemistry*; Ellis Horwood: New York, 1991.

(2) (a) *Molecular Electronics*; Jortner, J., Ratner, M., Eds.; Blackwell: Oxford, 1997. (b) Ball, P. *Nature* **2000**, *406*, 118−120.

(3) (a) de Silva, A. P.; Dixon, I. M.; Gunaratne, H. Q. N.; Gunnlaugsson, T.; Maxwell, P. R. S.; Rice, T. E. *J. Am. Chem. Soc.* **1999**, *121*, 1393−1394. (b) de Silva, A. P.; Gunaratne, H. Q. N.; McCoy, C. P. *Nature* **1993**, *364*, 42−44. (c) Debreczeny, M. P.; Svec, W. A.; Wasielewski, M. R. *Science* **1996**, *274*, 584−587. (d) Kawai, S. H.; Gilat, S. L.; Lehn, J.-M. *J. Chem. Soc., Chem. Commun*. **1994**, 1011−1013. (e) Ji, H.-F.; Dabestani, R.; Brown, G. M. *J. Am. Chem. Soc.* **2000**, *122*, 9306−9307. (f) Hopfield, J. J.; Onuchic, J. N.; Beratan, D. N. *Science* **1988**, *241*, 817−820. (g) Raymo, F. M.; Giordani, S. *J. Am. Chem. Soc.* **2001**, *123*, 4651−4652. (h) Credi, A.; Balzani, V.; Langford, S. J.; Stoddart, J. F. *J. Am. Chem. Soc*. **1997**, *119*, 2679−2681.

(4) Balzani, V. *Tetrahedron* **1992**, *48*, 10443−10514.

(5) (a) Balzani, V.; Credi, A.; Raymo, F. M.; Stoddart, J. F. *Angew. Chem., Int. Ed.* **2000**, *39*, 3349−3391. (b) *Biological Aspects of Fullerenes*, Wilson S. R., Kadish K., Ruoff, R., Eds.; John-Wiley: New York, 2000.

(6) Keefe, M. H.; Benkstein, K. D.; Hupp, J. T. *Coord. Chem. Rev.* **2000**, *205*, 201−228.

(7) De Silva, A. P.; McClenaghan, N.; McCoy, C. P.; Balzani, V. Logic Gates. In *Electron Transfer in Chemistry*; Wiley-VCH: Weiheim, Germany, 2001; Vol. 5, pp 156−185.

(8) Luo, Y.; Collier, C. P.; Jeppesen, J. O.; Nielsen, K. A.; Delonno, E.; Ho, G.; Perkins, J.; Tseng, H. R.; Yamamoto, T.; Stoddart, J. F.; Heath, J. R. *Chem. Phys. Chem.* **2002**, *3*, 519−525.

(9) (a) Gust, D.; Moore, T. A.; Moore, A. L. *Acc. Chem. Res*. **2001**, *34*, 40−48. (b) Wasielewski, M. R. *Chem. Rev*. **1992**, *92*, 435−461. (c) Meyer, T. J. *Acc. Chem. Res*. **1989**, *22*, 163−170.

(10) Gust, D.; Moore, T. A.; Moore, A. L. *Acc. Chem. Res.* **1993**, *26*, 198−205.

(11) Sacriftci, N. S.; Smilowitz, L.; Heeger, A. J.; Wudl, F. *Science* **1992**, *258*, 1474−1476.

(12) Williams, R. M.; Koeberg, M.; Lawson, J. M.; Yi-Zhong, A.; Rubin, Y.; Paddon-Row, M. N.; Verhoeven, J. W. *J. Org. Chem*. **1996**, *61*, 5055−5062.

(13) Guldi, D. M.; Maggini, M.; Scorrano, G.; Prato, M. *J. Am. Chem. Soc*. **1997**, *119*, 974−980.

(14) (a) Gust, D.; Moore, T. A.; Moore, A. L. *Res. Chem. Intermed*. **1997**, *23*, 621−651. (b) Balbinot, D.; Atalick, S.; Guldi, D. M.; Hatzimarinaki, M.; Hirsch, A.; Jux, N. *J. Phys. Chem. B* **2003**, *107*, 13273−13279

(15) (a) Imahori, H.; Yamada, K.; Hasegawa, M.; Taniguchi, S.; Okada, T.; Sakata, Y. *Angew. Chem., Int. Ed.* **1997**, *36*, 2626−2629. (b) Imahori, H.; Tamaki, K.; Guldi, D. M.; Luo, C.; Fujitsuka, M.; Ito, O.; Sakata, Y.; Fukuzumi, S. *J. Am. Chem. Soc*. **2001**, *123*, 2607−2617. (c) Imahori, H.; Mori, Y.; Matano, J. *J. Photochem. Photobiol., C: Photochem. Rev.* **2003**, *4*, 51−83.

(16) Bell, T. D. M.; Smith, T. A.; Ghiggino, K. P.; Ranasinghe, M. G.; Shephard, M. J.; Paddon-Row, M. N. *Chem. Phys. Lett.* **1997**, *268*, 223−228.

(17) (a) Da Ros, T.; Prato, M.; Guldi, D. M.; Alessio, E.; Ruzzi, M.; Pasimeni, L. *Chem. Commun*. **1999**, 635−636. (b) Da Ros, T.; Prato, M.; Guldi, D. M.; Ruzzi, M.; Pasimeni, L. *Chem.—Eur. J.* **2001**, *7*, 816−827. (c) Guldi, D. M.; Luo, C.; Da Ros, T.; Prato, M. Dietel, E.; Hirsch, A. *Chem. Commun*. **2000**, 375−376. (d) Guldi, D. M.; Luo, C.; Swartz, A.; Scheloske, M.; Hirsch, A. *Chem. Commun.* **2001**, 1066−1067.

(18) Wilson, S. R.; MacMahon, S.; Tat, F. T.; Jarowski, P. D.; Schuster, D. I. *Chem. Commun.* **2003**, 226−227

(19) Diederich, F.; Lopez, M. G. *Chem. Soc. Rev*. **1999**, *28*, 263−277.

(20) Piotrowiak, P. *Chem. Soc. Rev.* **1999**, *28*, 143−150.

(21) (a) D'Souza, F.; Deviprasad, G. D.; El-Khouly, M. E.; Fujitsuka, M.; Ito, O. *J. Am. Chem. Soc.* **2001**, 123, 5277−5284. (b) D'Souza, F.; Deviprasad, G. R.; Zandler, M. E.; Hoang, V. T.; Arkady, K.; Van Stipdonk, M.; Perera, A.; El-Khouly, M. E.; Fujitsuka, M.; Ito, O. *J. Phys. Chem. A* **2002**, *106*, 3243−3243. (c) D'Souza, F.; Deviprasad, G. R.; Zandler, M. E.; El-Khouly, M. E.; Fujitsuka, M.; Ito, O. *J. Phys. Chem. B* **2002**, *106*, 4952−4962.

(22) Guldi, D. M.; Ramey, J.; Martinez-Diaz, M. V.; de la Escosura, A.; Torres, T.; Da Ros, T.; Prato, M. *Chem. Commun*. **2002**, 2774−2775.

(23) (a) Watanabe, N.; Kihara, N.; Furusho, Y.; Takata, T.; Araki, Y.; Ito, O. *Angew. Chem., Int. Ed.* **2003**, *42*, 681−683. (b) Sandanayaka, A. S.

D.; Watanabe, N.; Ikeshita, K.; Araki, Y.; Kihara, N.; Furusho, Y.; Ito, O.; Takata, T. *J. Phys. Chem. B* **2004**, *109*, 2516−2525.

(24) Guldi, D. M.; Scheloske, M.; Dietel, E.; Hirsch, A.; Troisi, A.; Zerbetto, F.; Prato, M. *Chem.*−*Eur. J.* **2003**, *9*, 4968−4979.

(25) Sandanayaka, A. S. D.; Sasabe, H.; Araki, Y.; Kihara, K.; Furusho, Y.; Takata, T.; Ito, O. *Aust. J. Chem.*, in press.

(26) (a) Maggini, M.; Karlsson, A.; Scorrano, G.; Sandona, G.; Farnia, G.; Prato, M. *J. Chem. Soc., Chem. Commun.* **1994**, 589−590. (b) Prato, M.; Maggini, M.; Giacometti, C.; Scorrano, G.; Sandona, G.; Farnia, G. *Tetrahedron* **1996**, *52*, 5221−5234.

(27) (a) Fujitsuka, M.; Ito, O.; Imahori, H.; Yamada, K.; Yamada, Y.; Sakata, Y. *Chem. Lett*. **1999**, 721−722. (b) Imahori, H.; Tamaki, K.; Araki, Y.; Sekiguchi, Y.; Ito, O.; Sakata, Y.; Fukuzumi, S. *J. Am. Chem. Soc.* **2002**, *124*, 5165−5174. (c) Imahori, H.; Sekiguchi, Y.; Kashiwagi, Y.; Sato, T.; Araki, Y.; Ito, O.; Yamada, H.; Fukuzumi, S. *Chem.*−*Eur. J.* **2004**, *10*, 3184−3196.

(28) (a) D'Souza, F.; Zandler, M. E.; Smith, P. M.; Deviprasad, G. R.; Arkady, K.; Fujitsuka, M.; Ito, O. *J. Phys. Chem. A* **2002**, *106*, 649−656. (b) D'Souza, F.; Zandler, M. E.; Smith, P. M.; Deviprasad, G. R.; Arkady, K.; Fujitsuka, M.; Ito, O. *J. Org. Chem.* **2002**, *67*, 9122−9229.

(29) Fujitsuka, M.; Tsuboya, N.; Hamasaki, R.; Ito, M.; Onodera, S.; Ito, O.; Yamamoto, Y. *J. Phys. Chem. A* **2003**, *107*, 1452−1458.

(30) Imahori, H.; Yamada, H.; Nishimura, Y.; Yamazaki, I.; Sakata, Y. *J. Phys. Chem. B* **2000**, *104*, 2099−2108.

(31) Furusho, Y.; Sasabe, H.; Natsui, D.; Murakawa, K.; Harada, T.; Takata, T. *Bull. Chem. Soc. Jpn*. **2004**, *77*, 179−185.

(32) Kihara, N.; Tachibana, Y.; Kawasaki, H.; Takata, T. *Chem. Lett*. **2000**, 506−507.

(33) Weller, A. *Z. Phys. Chem. Neue Folge* **1982**, *133*, 93−98.

(34) Luo, C.; Fujitsuka, M.; Watanabe, A.; Ito, O.; Gan, L.; Huang, Y. Huang, C.-H. *J. Chem. Soc., Faraday Trans.* **1998**, *94*, 527−532.

(35) Araki, Y.; Yasumura, Y.; Ito, O. *J. Phys. Chem. B* **2005**, *109*, 9843−9848.

(36) (a) Yam, V. W.; Lee, V. W.; Cheung, K. *J. Chem. Soc., Dalton Trans*. **1997**, 2335−2339 (b) Sohn, Y. S.; Hendrickson, D. N.; Gray, H. B. *J. Am. Chem. Soc*. **1971**, *93*, 3603−3612.

(37) (a) Sension, R. J.; Phillips, C. M.; Szarka, A. Z.; Romanow, W. J.; McGhie, A. R.; McCauly, J. P., Jr.; Smith A. B., III; Hochstrasser, R. M. *J. Phys. Chem*. **1991**, *95*, 6075−6078. (b) Ebbesen, T. W.; Tanigaki, K.; Kuroshima, S. *Chem. Phys. Lett*. **1991**, *181*, 501−504. (c) Lee, M.; Song, O.-K.; Seo, J.-C.; Kim, D.; Suh, Y. D.; Jin, S. M.; Kim, S. K. *Chem. Phys. Lett*. **1992**, *196*, 325−329. (d) Watanabe, A.; Ito, O.; Watanabe, M.; Saito, H.; Koishi, M. *J. Chem. Soc., Chem. Commun.* **1996**, 117−118.

(38) (a) Sandanayaka, A. S. D.; Sasabe, H.; Araki, Y.; Furusho, Y.; Ito, O.; Takata, T. *J. Phys. Chem. A* **2004**, *108*, 5145−5155. (b) Sandanayaka, A. S. D.; Ikeshita, K.; Watanabe, N.; Araki, Y.; Furusho, Y.; Kihara, N.; Takata T.; Ito, O. *Bull. Chem. Soc. Jpn.* **2005**, *78*, 1008−1017.

(39) (a) Marcus, R. A. *J. Chem. Phys.* **1956**, *24*, 966−978. (b) Marcus, R. A. *J. Chem. Phys.* **1965**, *43*, 679−701. (c) Marcus, R. A.; Sutin, N. *Biochim. Biohys. Acta* **1985**, *811*, 265−322.

(40) Yamazaki, M.; Araki, Y.; Fujitsuka, M.; Ito, O. *J. Phys. Chem. A* **2001**, *105*, 8615−8622.

(41) Andersson, A.; Linke, M.; Chambron, J.-C.; Davidsson, J.; Heitz, V.; Sauvage, J.-P.; Hammarström, L. *J. Am. Chem. Soc.* **2000**, *122*, 3526−3528.

(42) (a) Ito, O.; Sasaki, Y.; Yoshikawa, Y.; Watanabe, A. *J. Phys. Chem*. **1995**, *99*, 9838−9842. (b) Ito, O. *Res. Chem. Intermed*. **1997**, *23*, 389−402. (c) Yahata, Y.; Sasaki, Y.; Fujitsuka, M.; Ito, O. *J. Photosci.* **1999**, *6*, 117−121.